Effect analysis of wooden fence width on wave transmission by SWASH model

To cite this article: T Mai *et al* 2023 *IOP Conf. Ser.: Mater. Sci. Eng.* **1294** 012026

Effect analysis of wooden fence width on wave transmission by SWASH model

T Mai[1,*], H T Dao[2], T T A Ngo[3], H H Pham[1], Y Liu[4]

[1] Hanoi University of Civil Engineering, Vietnam
[2] Hanoi University of Natural Resources and Environments, Vietnam
[3] Thuyloi University, Vietnam
[4] Norwegian University of Science and Technology, Norway

[*] Correspondence: trimc@huce.edu.vn

Abstract. Wooden fences, a permeable structure, have become a nature-based solution for supporting traditional structures to restore mangrove forests along the Mekong deltaic coasts. Even though prior studies have explored a number of hydraulic functions of these fences, an in-depth investigation into the influence of fence width on wave dissipation and damping is needed to consider. Therefore, this paper employs a numerical approach to thoroughly examine the impact of fence width on wave damping. The findings illustrate the substantial role of fence width in governing the dissipation of incoming waves. The correlation between the transmission coefficient and the fence width is established. This relationship also concludes that the larger the fence thicknesses, the lower the transmission coefficients. Notably, the study also identifies that the transmission coefficient experiences a slight decline beyond a certain width threshold.
Keywords: wooden fence, wave transmission, Mekong Delta, mangroves, relative fence thickness.

1. Introduction

The Mekong deltaic coast is known as one of the largest deltas in the world, with a rich diversity of ecosystems, including mangroves. Mangrove is the natural defense and protection for the coast because it morphs massively and naturally coastal sediment along the coast. Furthermore, mangrove forest provides a lively environment for local animal and livelihood communities.

However, due to climate change and sea level rise, the mangrove belt along the coast in the Mekong Delta provinces has been seriously degraded [1,2]. As a result, the retreatment of the mangrove belt has led to an increasing rate of coastal erosion. There have also been a number of hard/gray construction solutions applied, such as hollow pillar breakwaters and centrifugal concrete pile walls for breaking waves, to protect and prevent the coast from erosion. However, these solutions are oddly expensive and harmfully environmental. Additionally, gray structures often break the equilibrium of morphodynamics, such as wave, flow, and sediment transport.

On the other hand, planting young mangrove trees for gradual restoration and maintaining the mangrove belt is a nature-based solution currently applied to these damaged areas [3]. Furthermore, building soft walls, e.g., wooden fences, for waves and currents reduction and sediment acceleration, gives an important job in the work of supporting young mangroves. This solution also supports the old mangrove forests at the side already protected by the sea dikes.

In order to widely apply wooden fences for wave load reduction to mangrove forests, determining the influence of the wooden fence and wave parameters on the wave-damping efficiency by formulas or relational lines is essential today. In the context of designing wooden fences, Dao et al. (2020, 2021) [4,5] studied wave transmission over different fence thicknesses ranging from 1.4 m to 3.6 m, scaled from laboratory data. This study approached a numerical model to assess the relationship of wave transmission coefficient ($K_T = H_T/H_I$, with H_T and H_I are the transmission and incident wave heights, respectively) and the relative thicknesses with wave height (B/H). However, the result only presents wave height reduction occurred when low incoming wave heights impact the fences. For a similar context of thicknesses, wave reduction over the mangrove's width was studied in the previous research, i.e., Phan et al. (2019) [6] for laboratory study and Dao et al. (2018, 2021) [4,7] for numerical studies. However, this study only focused on the assessment of transmission for the non-linearity of waves. In more recent studies, Shu et al. (2023) [8] studied wave energy reduced by artificial bamboo fences in the laboratory scales, concluding the effect of wave transmission on the wave steepness and the non-linearity, but the fence's thickness on wave transmission is still hindered. Mancheno et al. (2023) [9] and Qu et al. (2023) [10] applied the open-source non-hydrostatic model to study wave attenuation over emergent rigid cylinders, which consider wooden fences and vegetations, respectively. While Qu et al. (2023) focused on using a numerical model (NHWAVE) to get a further understanding of vegetation densities and width on wave transmission, Mancheno et al. (2023) then used the SWASH model to study the effect of distance between cylinders on wave reductions.

Further understanding of relationships between fence widths and wave transmissions still needs to be carried out since a fence's design should be carefully considered for both efficiency and construction cost. Therefore, in this study, the main objective is to identify the relationship between wave transmission and the thickness of the fence relative to wavelength. An open-source model, SWASH, developed by Delft University of Technology, is used to simulate wave-fence interaction and assess the wave transmission coefficient with relative fence thicknesses. This paper will present the results of research to evaluate the effect of fence width on wave propagation through wooden fences through a mathematical model.

2. Methodology

2.1 SWASH model

SWASH model is an open-source model based on the nonlinear shallow water equations [11] that can simulate the multidimensional time-domain model for non-hydrostatic, free surface flow. The SWASH model can also consider shallow processes in the near-shore, such as breaking, reflection, and diffraction [12–15]. SWASH model is also applied for further research on wave-runup and overtopping [16] and prediction of wave-runup on a coral-reef bed [17]. Further study on the improvement of wave height prediction in the near-shore is also carried out by Umesh, P and Behera, M (2021) [18].

The government equations used to simulate waves traveling through a section perpendicular to the shore are as follows:

$$\frac{\partial u}{\partial x} + \frac{\partial w}{\partial z} = 0 \tag{1}$$

$$\frac{\partial \eta}{\partial t} + \frac{\partial}{\partial x}\int_{-d}^{\eta} u dz = 0 \tag{2}$$

$$\frac{\partial w}{\partial t} + \frac{\partial uw}{\partial x} + \frac{\partial ww}{\partial z} + \frac{1}{\rho}\frac{\partial (P_{nh})}{\partial z} + \frac{\partial \tau_{zz}}{\partial z} + \frac{\partial \tau_{zx}}{\partial x} = 0 \tag{3}$$

$$\frac{\partial u}{\partial t} + \frac{\partial uu}{\partial x} + \frac{\partial wu}{\partial z} + \frac{1}{\rho}\frac{\partial (P_h + P_{nh})}{\partial x} + \frac{\partial \tau_{xz}}{\partial z} + \frac{\partial \tau_{xz}}{\partial x} = 0 \tag{4}$$

where x and z are the horizontal and vertical directions in Decade coordinate, respectively; u and w are the horizontal and vertical particle velocities, respectively; η is the water elevation; t is the time; P_h and P_{nh} are the hydrostatic and non-hydrostatic pressures, respectively; the bottom stress follows a quadratic friction law and expressed as:

$$\tau_b = c_f \frac{U|U|}{\eta+d} \tag{5}$$

where u is the average depth velocity and c_f is the friction coefficient based on Manning:

$$c_f = \frac{n^2 g}{d^{1/3}} \tag{6}$$

In this study, a crossed profile was set in Figure 1, defined with a slope to create a breaking point for waves before entering the horizontal zone. Note that the profile mimics the gentle slope (approximately 1:1000) found in the Mekong deltaic coast. Wave inputs were set at the west side of the profile. At the east side, a 75m-sponger layer was set to absorb most of the reflection from both short- and longwaves. A spatial resolution (Δx) of 0.05, which is approximately $L_p/100$ (with L_p is the peak wavelength), was applied. The background viscosity of 3.10^{-4} was put in the model. A constant friction coefficient of 0.02 was also added. Other settings were set as default [11].

An assumption is that the bamboo poles are rigid in the SWASH model simulation. The vegetation implementation model was used in order to simulate wooden fences with three main parameters of a cylinder, including density (number of cylinders per area), diameter, and bulk drag coefficient [4,7]. Irregular wave characteristics include significant wave height and peak period applied at the boundary (left side of the profile, Figure 1). When waves come into contact with the fence (at x = 125 m, Figure 1), transmission wave height (H) can be calculated as:

$$\frac{H}{H_0} = \frac{1}{1+\tilde{\beta}x} \tag{7}$$

where, $\tilde{\beta}$ is the dissipation parameter expressed by Suzuki et al. (2019) [19] after implementing a horizontal component of wave forces to a cylinder from the study of Mendez and Losada (2004) [20]:

$$\tilde{\beta} = \frac{1}{3\sqrt{\pi}} \overline{C_D} DNH_0 k \frac{sinh^3(k\alpha H_f)+3\,sinh(k\alpha H_f)+cosh^3(k\alpha H_f)-3\,cosh(k\alpha H_f)+2}{[sinh(2kd)+2kd]sinh\,(kd)} \tag{8}$$

in which αH_f (m) is the submerged depth of the fence and k is the wave number. As seen in equation (8), transmission wave height is influenced by the three main parameters mentioned above. In Figure 1b, wooden fence settings in the model are expressed with horizontal and vertical orientations representing for vertical and horizontal forces, respectively. Note that the orientation of the fence is the showcase for interpretation of equation (8).

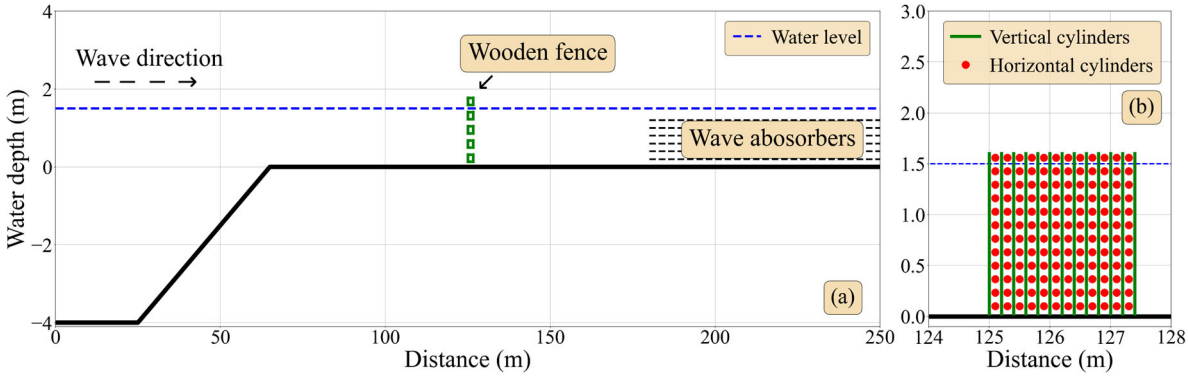

Figure 1. (a) Simulation profile in SWASH; (b) Wooden fence formulation with vertical (green line) and horizontal cylinders (red dot).

2.2. Field data and scenarios

In this study, wave and wooden fence characteristics were mimicked from field measurements in Nhat Mat, Bac Lieu, Vietnam [21] (Figure 2). Waves, including wave heights and wave periods, were

obtained from measurements in front and behind the fence (Figure 2b), while only fence thicknesses were measured with two values of 0.8 and 1.6 m.

Due to the high dissipation environment for waves during propagation to the shore, the wooden fence was set at x = 125 m, far enough from the breaking point, as shown in Figure 1. Additionally, sea dikes in the field create unpredictable reflections due to longwaves. Therefore, sponger layers were set instead of dike to reduce as much complexity as possible. Other parameters include a cylinder diameter (D) of 0.02 m, a density of 636 cylinders per m^2 equal to about 80% porosity, and a bulk drag coefficient inherited from Dao et al. (2020) 2.0 for every scenario. Following Dao et al. (2020) [5], the relation between cylinder gap, s, and diameter D is calculated as 1.0, and it is suitable for this study to use because of the similar application. Also, only one fence height was used, 1.6 m. To assess the thickness dependency, several fence widths were set, ranging from 0.8 to 2.4 m. However, note that only one density was used to necessarily reduce the complexity of the assessment.

Table 1. Simulation scenarios.

Wave height (H_s, m)	Wave period (T_p, s)	Water depth (d, m)	Fence width (B, m)
0.39	5.57	1.53	0.8, 1.0, 1.2, 1.4, 1.6, 1.8, 2.0, 2.4
0.42	6.37	1.46	0.8, 1.0, 1.2, 1.4, 1.6, 1.8, 2.0, 2.4
0.52	7.31	1.58	0.8, 1.0, 1.2, 1.4, 1.6, 1.8, 2.0, 2.4
0.66	8.41	1.44	0.8, 1.0, 1.2, 1.4, 1.6, 1.8, 2.0, 2.4

As can be seen in Table 1, four different wave heights, wave periods, and water depths were applied to the input boundary. For each fence thickness, four-wave characteristics were used. All scenarios are presented in Table 1.

Figure 2. Fence location where field measurements were obtained (Dao et al. 2021) [4]: (a) Mekong Delta; (b) Nha Mat, Bac Lieu, Mekong.

3. Results and discussions

In this section, wave heights and surface elevations are presented as a part of the result of wave transformation over the profile. Next, the relationships between wave transmission coefficient and the relative fence thickness with wavelength and wave height are shown to assess the roles of width on wave reduction.

3.1 Wave transformation over the profile

Figure 3 presents standing wave heights in different scenarios. Wave propagation in each case illustrates different stages of a wave during its traveling to the near-shore. In the showcases in Figure 3, breaking waves appear at the early stage when water depth reduces from 4 m to about 2 m at x = 50 m to 80 m. However, the higher the incoming waves, the more wave breaking, as shown in Figures 3a&b. Smaller waves presented in Figure 3c&d slightly break after a short delay since these waves enter the shallow area lately.

Due to the appearance of the wooden fence at x = 125 m (Figure 3e), wave heights in all showcases are reduced by about 50% of their energies after reflection. Also, most wave energies are absorbed by the sponger layers. Therefore, transmission waves seem to have minor impacts from reflections at the east side.

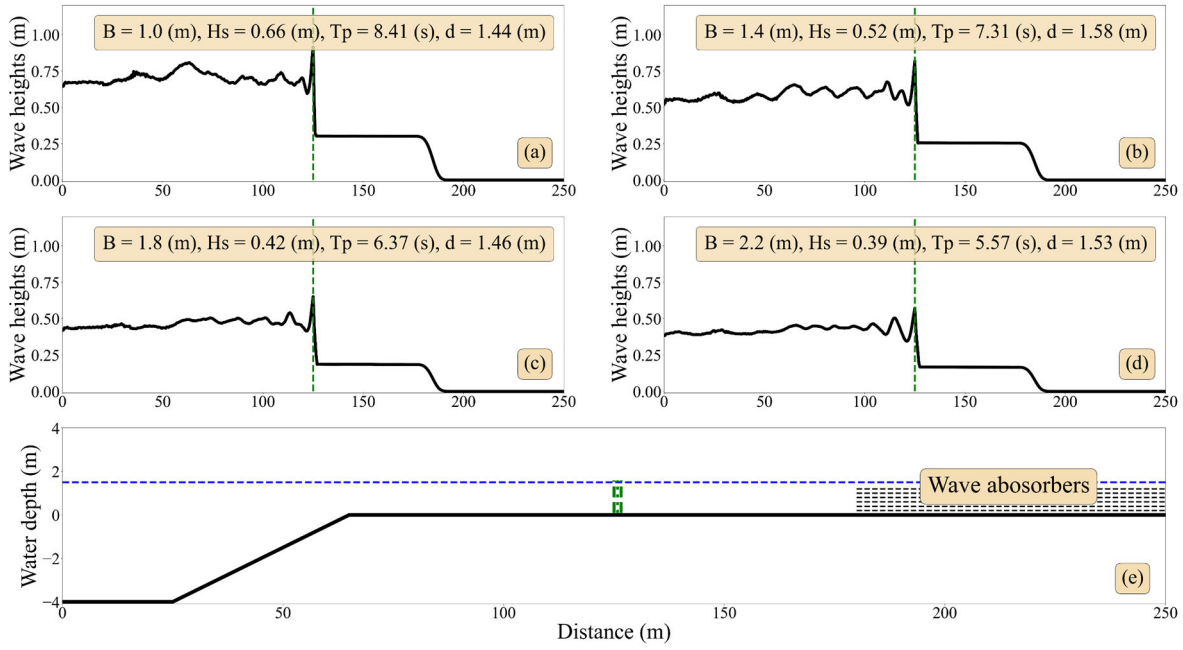

Figure 3. Standing waves over the fences.

Additionally, surface elevations and wave spectrum at locations in front and behind the fence of all showcases in Figure 3 are presented in Figure 4. For each case, surface elevations behind the fence are significantly reduced for larger waves (Figures 4b&d) but slightly decreased for smaller waves (Figures 4e & g). Yet, the porosity of wooden fences was set at about 85%, and the wave damped by them is highly presented. For example, all transmission wave spectrums (blue line) in the showcases (Figure 4a,c,f,h) are much lower than incoming waves (red line).

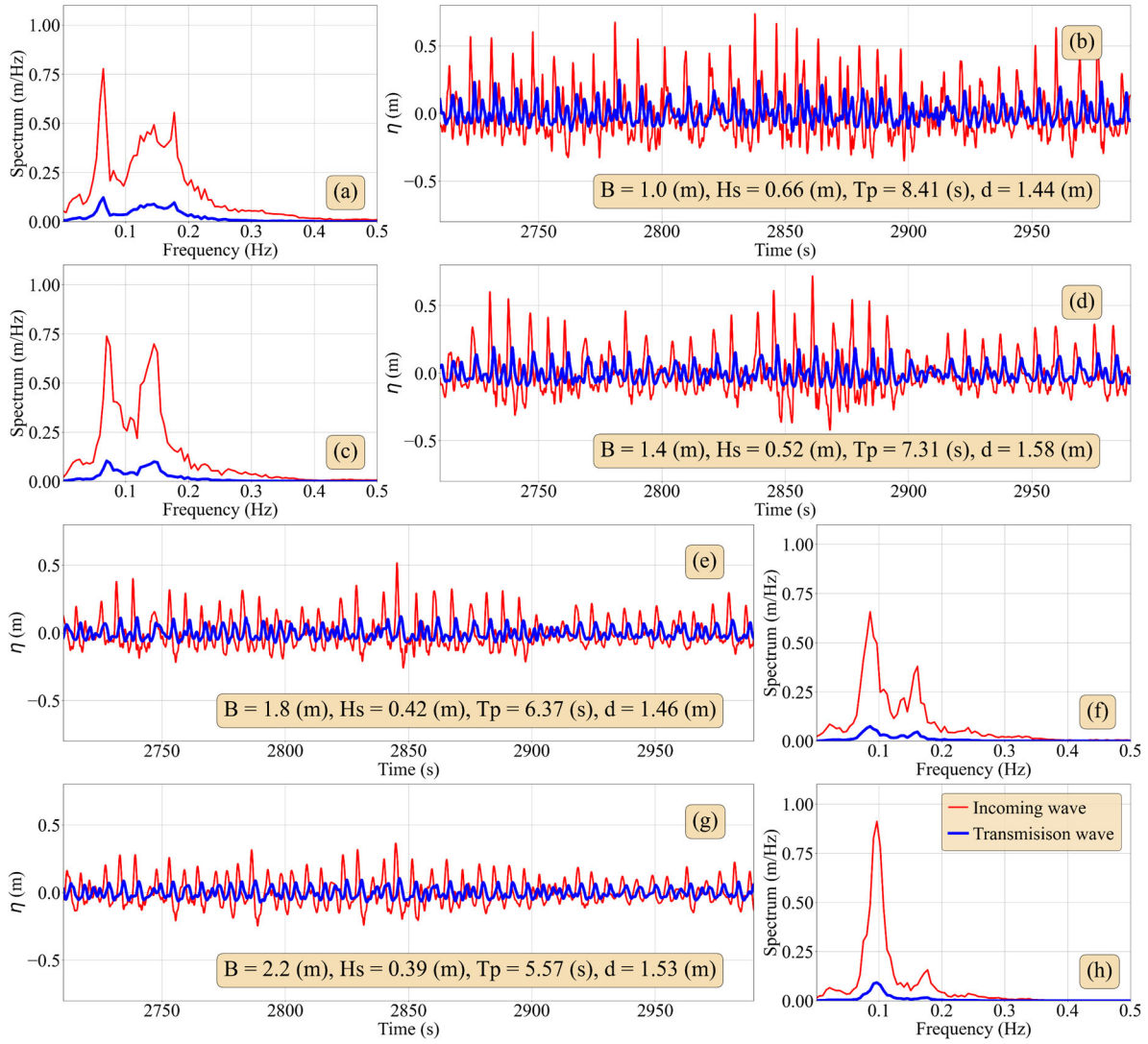

Figure 4. Surface elevation (b, d, e, g) and wave spectrum (a, c, f, h).

3.2 Wave transmission and fence thicknesses

In this section, the influence of fence thickness is presented in Figure 5 and Figure 6. The wave transmission coefficient (K_t) is plotted against two dimensionless parameters, which are expressed as:

$$K_t = \frac{H_t}{H_i} \tag{9}$$

where H_t and H_i are transmission and incoming wave heights, respectively.

In Figure 5, the relative fence thickness with incoming wave height is plotted against the transmission coefficient, and this plot is compared with the previous study [4]. The scatters from Figure 5 illustrate the reduction trend of incoming waves, indicating that larger waves tend to be damped more significantly and even more for the larger fence thickness.

The transmission coefficients in this study (red circles) value from 0.3 to 0.5 with the B/H_i from 1 to 4. These scatters interestingly match the data from Dao et al. (2021) [4] for the same range of B/H_i. The gap of K_t between the two studies can be interpreted by the difference of porosities applied. Furthermore, the fit line (dashed line) from this study is well-fit with Dao et al. (2021) [4] showing an influence of fence thickness on incoming wave height. The two scatters and the fit-line are interestingly matched at

a *B/Hi* value of about 4. This can be explained by the fact that the larger thicknesses dissipate most of the wave, and at a certain point, wave reduction reaches the same proportion in Dao et al. (2021) with lower porosity. The larger the thickness is, the higher the wave is damped.

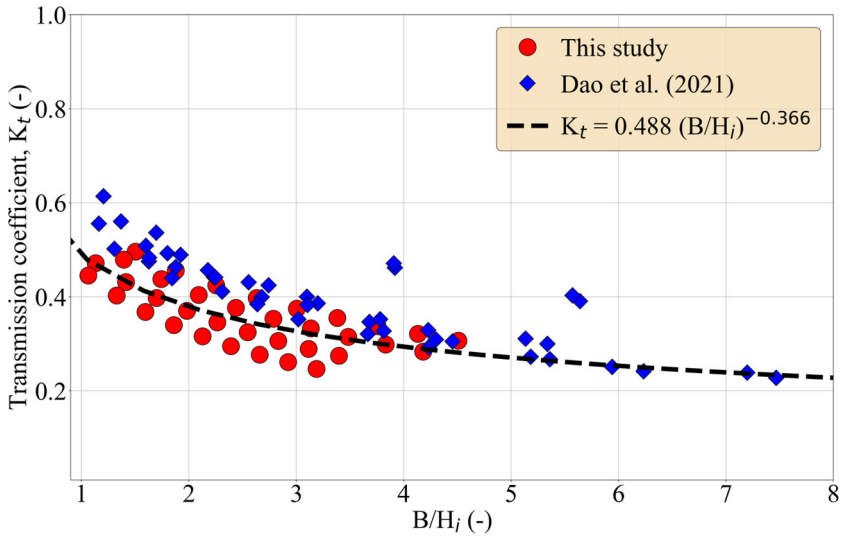

Figure 5. Relative fence thickness with incoming wave height and transmission coefficient with additional data from Dao et al. (2021) [4].

Since the influence of thicknesses on incoming wave heights is shown in Figure 5, the impact of this characteristic on wavelength, directly calculated from wave period and water depth, is indicated in Figure 6. Since water depths for every scenario are merely similar, it is acceptable to ignore the depth effects. In Figure 6, the larger waves (higher period) tend to be damped more than smaller waves, such as K_t ranges from 0.3 to 0.5 for B/L_i from 0.02 to 0.12.

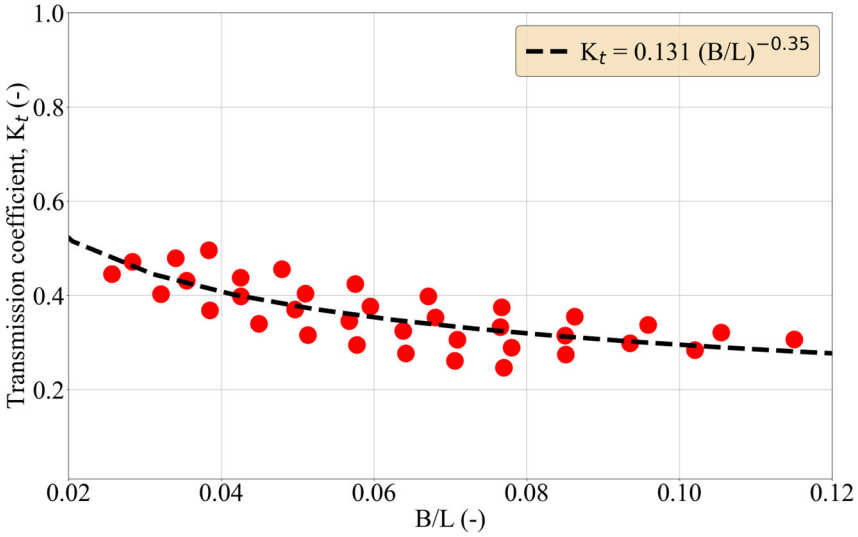

Figure 6. Relative fence thickness with wavelength and transmission coefficient.

Both results in Figures 5 and 6 have power fit lines that give an idea for wooden fence designs. As a result, the optimization for fence thicknesses can be indicated based on those two power expressions.

4. Conclusions

This study indicates the influence of fence thickness on wave damping, and the efficiency of wave reduction based on different widths can be indicated from the simulation results.

The SWASH model has been applied in previous studies, such as Dao et al. (2018, 2021) [4,7], showing a capability for simulating wave-fence interactions. The results show that wave heights are reduced from 30% to 70% of heights after contacting wooden fences. The large range of wave reduction also illustrates the dependency of wave damping on fence thicknesses. Additionally, the relations of wave transmissions and the relative fence thicknesses are presented as a decreased trend. In detail, the larger wave reduction often appears with the high value of the dimensionless parameters B/H_i and B/L_i. These results conclude that waves tend to be highly damped due to larger fence width. Note that other influencing parameters, such as water depth and reflection, are made as minimum as possible.

Furthermore, the other stages of wave-fence interactions, including wave reflection and dissipation, are left out due to the complexity of the fence's characteristics. For example, the high reflection often occurs for higher density or lower porosity, resulting in the difficulty of predicting the dissipation rate inside a wooden fence.

References

[1] Anthony EJ, Brunier G, Besset M, Goichot M, Dussouillez P and Nguyen VL 2015 Linking rapid erosion of the Mekong River delta to human activities. *Sci Rep* **5** 14745.
[2] Báo Tài nguyên và Môi trường (Vietnamese) 2018 Đồng bằng sông Cửu Long: Xói lở bờ biển bủa vây. n.d.
[3] Mazda Y, Magi M, Kogo M and Hong PN 1997 Mangroves as a coastal protection from waves in the Tong King delta, Vietnam. *Mangroves and Salt Marshes* **1** 127–35.
[4] Dao HT, Hofland B, Suzuki T, Stive MJF, Mai T and Tuan LX 2021 Numerical and small-scale physical modelling of wave transmission by wooden fences.
[5] Dao HT, Hofland B, Stive MJF and Mai T 2020 Experimental assessment of the flow resistance of coastal wooden fences. Water (Basel) **12**:1910.
[6] Phan KL, Stive MJF, Zijlema M, Truong HS and Aarninkhof SGJ 2019 The effects of wave non-linearity on wave attenuation by vegetation. *Coastal Eng.* **147**:63–74.
[7] Dao T, Stive MJF, Hofland B and Mai T 2018 Wave Damping due to Wooden Fences along Mangrove Coasts. *J Coast Res* **34**:1317–27. https://doi.org/10.2112/JCOASTRES-D-18-00015.1.
[8] Shu A, Zhu J, Cui B, Wang L, Zhang Z and Pi C. 2023 Coastal wave-energy attenuation by artificial wooden fences deployed for mangrove restoration: an experimental study. *Front Mar Sci* **10**:1165048.
[9] Mancheno AG, Reniers A and Suzuki T 2023 Optimising the wave attenuation of bamboo fences using the numerical wave model SWASH. *J. Coastal Hydr. Struct.* **3**, Paper 27.
[10] Qu K, Lan GY, Sun WY, Jiang CB, Yao Y, Wen BH, et al. 2021 Numerical study on wave attenuation of extreme waves by emergent rigid vegetation patch. *Ocean Eng.* **239**:109865.
[11] Zijlema M, Stelling G and Smit P. 2011 SWASH: An operational public domain code for simulating wave fields and rapidly varied flows in coastal waters. *Coastal Eng.* **58** 992–1012.
[12] Smit P, Zijlema M and Stelling G. 2013 Depth-induced wave breaking in a non-hydrostatic, near-shore wave model. *Coastal Eng*. **76** 1–16.
[13] Zijlema M and Stelling GS. 2005 Further experiences with computing non-hydrostatic free-surface flows involving water waves. *Int J Numer Methods Fluids* **48** 169–97
[14] Zijlema M. Modelling wave transformation across a fringing reef using SWASH. ICCE 2012: Proc. 33rd Int. Conf. Coastal Eng.g (Santander, Spain, 1-6 July 2012)
[15] Rijnsdorp DP, Smit PB and Zijlema 2012 M. Non-hydrostatic modelling of infragravity waves using SWASH. *Coastal Engineering Proceedings* **1** 27.
[16] Henderson CS, Fiedler JW, Merrifield MA, Guza RT and Young AP 2022 Phase resolving runup and overtopping field validation of SWASH. *Coastal Eng*. **175** 104128.

https://doi.org/https://doi.org/10.1016/j.coastaleng.2022.104128.
[17] Liu Y, Liao Z, Fang K and Li S. 2021 Uncertainty of wave runup prediction on coral reef-fringed coasts using SWASH model. *Ocean Eng.* **242** 110094. https://doi.org/https://doi.org/10.1016/j.oceaneng.2021.110094.
[18] Umesh PA and Behera MR. 2021 On the improvements in nearshore wave height predictions using nested SWAN-SWASH modelling in the eastern coastal waters of India. Ocean Eng. **236**:109550. https://doi.org/https://doi.org/10.1016/j.oceaneng.2021.109550.
[19] Suzuki T, Hu Z, Kumada K, Phan LK and Zijlema M 2019 Non-hydrostatic modeling of drag, inertia and porous effects in wave propagation over dense vegetation fields. *Coastal Eng*. **149**, 49 – 64, https://doi.org/10.1016/j.coastaleng.2019.03.011
[20] Mendez FJ and Losada IJ 2004 An empirical model to estimate the propagation of random breaking and nonbreaking waves over vegetation fields. *Coastal Eng.* **51**:103–18.
[21] Mai T, Dao T, Ngo A and Mai C 2019 Porosity Effects on Wave Transmission Through a Bamboo Fence. International Conference on Asian and Pacific Coasts, Springer 1413–8.